2016

Groundwater Recharge of a Landslide : An Isotopic and Meteorological Analysis

Bryan Allen
Portland State University

Undergraduate Honors' Thesis

Groundwater recharge of a landslide:

An Isotopic and meteorological analysis

Submitted to

Department of Geology
Portland State University

By

Bryan Allen
June 10st, 2016

ABSTRACT

Landslides pose a significant threat to property and personal injury, estimated at 3.5 billion dollars and 25-50 deaths per year respectively (Schuster, 1996). The triggers that cause landslides are well understood and include intense precipitation events, seismic shaking, destabilizing activities, and the over-steepening of slopes. However, these triggers were absent when the Silt Creek Landslide initiated, and determining this landslide's subsurface hydrologic conditions is the focus of this study. Located on the western slopes of the Cascade mountain range in Oregon and within an active logging area, the landslide reactivated during the summer of 2014 at a site that had previous landslides dating back to at least 1994. The area is underlain by poorly welded tuffs capped with basaltic flows. Considering the near-drought to drought conditions that existed 3 years' prior, it has a relatively high rate of slip of approximately 15 m/yr. On March 4th, 2016 I obtained twelve water samples from surface flow and springs on the landslide for isotope analysis of oxygen (^{18}O) and deuterium (D). Comparing the resultant mean, -10.09‰ $\delta^{18}O$, against well-defined linear elevation/ $\delta^{18}O$ relationships for western Oregon and

the Global Meteoric Water Line for $\delta^{18}O$ / δD the source of surface flow and groundwater likely originates from a pond above the head scarp. Analysis of precipitation data over a 42-year period prior to reactivation confirms the drought-like conditions existing at time of reactivation. These conditions align with the 'bathtub' model wherein an older landslide creates the conditions for repeated failures by aligning platy clay minerals such that the hydraulic conductivity is reduced to the point that a perched aquifer forms. This provides lubrication for subsequent landslides even during periods of low precipitation. Understanding the mechanisms operating on this landslide can inform future assessments of hazard and risk as well as appropriate mitigation strategies.

INTRODUCTION

Landslides pose a significant threat in terms of economic damage and personal injury. Landslides in the United States cause an estimated 3.5 billion dollars in damage and 25-50 deaths per year (Schuster, 1996). Landslide types are broadly categorized into bedrock based, such as rockfalls and topples, and soil based, which include slides and flows, and may exhibit a spectrum of intermixing attributes depending on composition and angle (Cruden and Varnes, 1996). Velocities range from the extremely slow rate of 0.06m/yr for slides to the extremely rapid rate of 3m/s for rockfall and debris flows (Ritter, 2011). The causes of slope failure are well established and include such typical triggers as intense precipitation events, seismic shaking, destabilization activities, and the over-steepening of slopes. Failure occurs when shear stresses exceed the internal shear strength threshold of a hillslope resulting in mass movement (Lambe and Whitman, 1969). Commonly this occurs when the pore pressures between individual sediment grains increase such that these grains begin to slide past or rotate over each other (Terzaghi, 1950). Increased pore pressure is commonly linked to precipitation events or longer term trends in groundwater levels, for example the wetter than average conditions that occurred over months to years that preceded the Oso landslide, which caused 43 deaths in Washington State in 2014 (Iverson, 2015). As precipitation infiltrates and contributes to sub-surface water flow the water table raises causing a decrease in effective normal stress and therefore a decrease in shear strength. Groundwater underneath a landslide may receive contributions that extend beyond the local recharge area and experience fluxes that reflect temporal variations beyond the near present.

Located approximately 7.5km due south of Mill City, OR within an active logging site, operated by Weyerhaeuser Columbia Timberlands, the Silt Creek Landslide resides in the Thomas Creek Watershed on the western slopes of the Cascade mountain rage (Figure 1). Reactivation of an older, 3.5km long landslide complex began approximately summer 2014, with a debris flow affecting the upper part of the landslide, and slower sliding occurring in the landslide's transport zone with an overall transport rate of ~15 m/yr. It is characterized as a composite earthflow-earthslide (Cruden and Varnes, 1996), with superimposed debris flows occurring near the head scarp. Earthflows-earthslides are defined as being composed of predominantly fine-grained soils while debris flows are composed mostly of coarser grained soils (Ritter, 2011). The summer of 2014 reactivation is unique in that the largest debris flows have occurred during the summer season under near-drought to drought conditions existing 3 years prior. Under these conditions, both groundwater recharge and pore pressure from sub-surface water flow are assumed to be typically low.

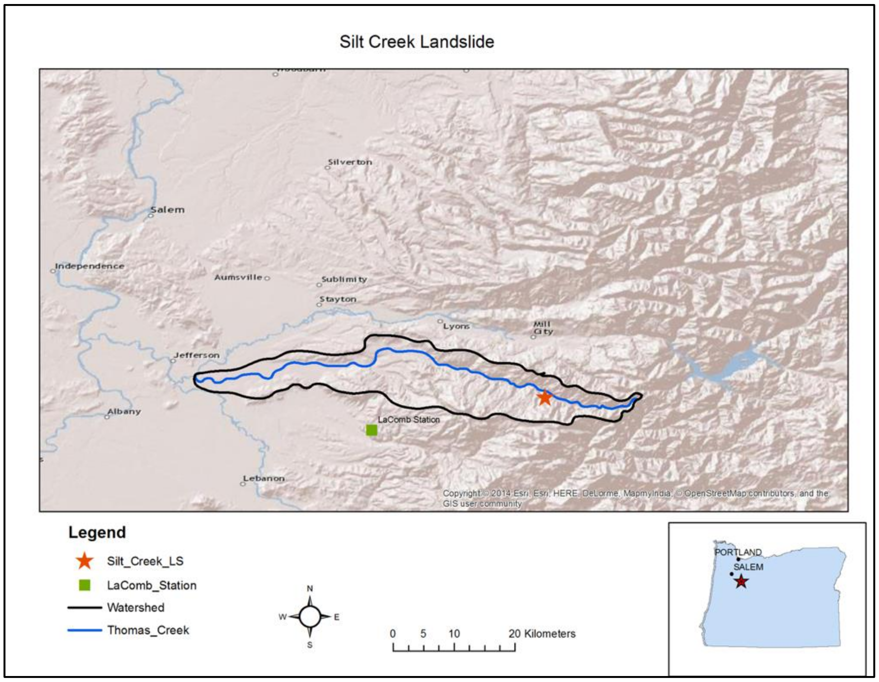

Figure 1. Overview map of study showing the location of Silt Creek Landslide (red star). Thomas Creek Watershed is outlined in black. Meteorological analysis was completed from data gathered at the climate station LaComb, identified as a green colored box.

Surface water flow contributes to groundwater by infiltrating vertically downward from the surface through the soil. The rate of infiltration is governed by the unsaturated hydraulic conductivity of the soil. Soil that has low permeability tends to have a low rate of infiltration due to it's a low unsaturated hydraulic conductivity. Surface flow at the study site originates as precipitation from air masses that form over the Pacific Ocean. As these air masses migrate eastward they raise in elevation up over the terrain. In doing so they cool, and precipitation falls when they reach a relative humidity of 100% (the dew point). The heavier isotopes of oxygen and hydrogen, ^{18}O and ^{2}H. precipitate out first, such that the higher elevations have isotopically lighter precipitation than do the lower elevations.

Oxygen and hydrogen isotopes in water can be useful for fingerprinting the sources of surface and groundwater. Isotopes are atoms of the same element with a different number of neutrons, and those with more neutrons have greater mass. This difference in mass results in a fractionation response that produces water with a unique isotopic composition signature. The following processes influence the isotopic composition of water: temperature (and therefore altitude), distance inland from a coast, timing and duration of precipitation, humidity levels, seasonal fluctuations, location, and humidity.

Considering the conditions present prior to the reactivation I hypothesize that regional groundwater beyond the surface extent of the landslide itself is infiltrating and destabilizing the slope. The primary goal of this thesis is to develop an understanding of the hydrological structure of the landslide through 1) using stable isotope analysis of oxygen and hydrogen, sampled from overland flow and springs on the landslide, to establish groundwater recharge elevation 2) estimating the area of groundwater recharge to the landslide based on recharge elevation and 3) analyzing past meteorological conditions contributing to the landslide reactivation.

GEOLOGIC SETTING

Residing in the heavily eroded Western Cascades, the Silt Creek Landslide occurs in deposits that have their origins ranging from the middle-to-late Eocene, approximately 40ma, to a lesser eruptive output at 17ma, and to High Cascade volcanism from 7.4ma to present (Orr, 2012). Predating the modern Cascades by 35ma the Western Cascades are centered on a more westerly arc than their modern counterparts, which is the result of the steeply descending Farallon Plate (a precursor to the modern day Juan De Fuca plate), and ongoing clockwise rotation of western Oregon (Wells, 2000). This produced "volcanogenic deposits of basalt and basaltic andesite, including flows and breccia, complexly interstratified with epiclastic and volcaniclastic deposits of basaltic to rhyodacitic composition" including "extensive rhyodacitic to andesitic ash-flow and air-fall tuffs, abundant lapilli tuff and tuff breccia, andesitic to dacitic mudflow (lahar) deposits, poorly bedded to well-bedded, fine- to coarse-grained tuffaceous sedimentary rocks, and volcanic conglomerate" (Walker and Macleod, 1991). Due to the age, amount of erosion, and deformation of the Western Cascades, the delineation between formations are complex, subtle, and at times not fully understood nor agreed upon. In light of this, principal formations listed are limited to widespread distribution and of diagnostic features. Therefore, primary formations associated with these deposits are the Breitenbush Tuffs, Mehama Volcanics and Quaternary landslide deposits (Figure 2). The majority of the Silt Creek landslide occurs in the Breitenbush Tuffs, with its head scarp possibly extending into the Mehama Volcanics.

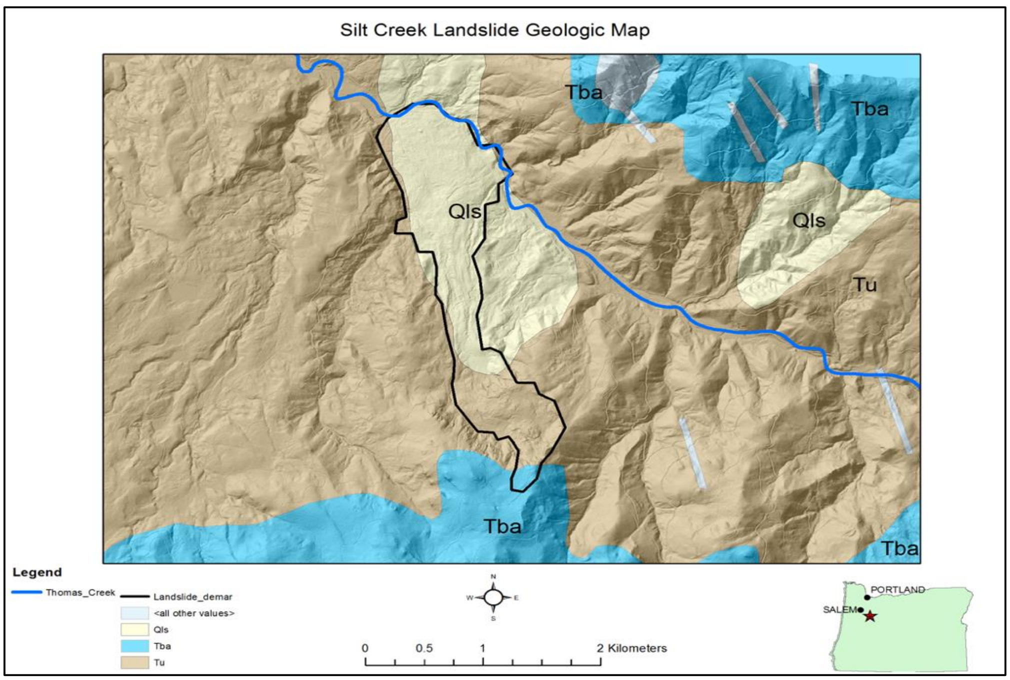

Figure 2. Geologic map of Silt Creek Landslide. The landslide boundary is in black. Geologic units are: Quaternary landslide deposits (Qls), Breitenbush Tuffs (Tu), and Mehama Volcanics (Tba). The blue line represents Thomas Creek.

Breitenbush Tuffs (Oligocene) (Tu)

Thayer (1939) identifies these tuffs as poorly to moderately welded, and suggests that they are the result of ignimbrite flows that form deposits approximately 580 to 915m thick. They are a ubiquitous layer throughout the North Santiam River region due to their thickness and colorization that ranges from pale green to light grey/olive. These tuffs are present throughout most of the lower elevations of the regions valleys (Hammond, 1976).

Mehama Volcanics (Miocene) (Tba)

The Mehama Volcanics is a small subset of the larger Sardine formation. These volcanics are comprised of thick layers of basaltic to dacitic lavas that reach upwards of 1300m in thickness (Thayer, 1939). Interbedded within these flows are lahars and tuffaceous rocks. Rocks of this unit are identifiable as porphorytic with plagioclase phenocrysts (White, 1980). The unit includes flow breccia, olivine andesite, basaltic-andesite, and basalt. This resistant formation is constrained to ridges and ridge-tops.

Quaternary Landslide Deposits (Qls)

Deposits are composed of "Unstratified mixtures of fragments of adjacent bedrock…Largest slides and debris flows occur where thick sections of basalt and andesite flows overlie clayey tuffaceous rocks." (Walker and Macleod, 1991)

Structurally, the Silt Creek Landslide lies between the Mehama anticline to the West and the Sardine syncline to the East. To the Southeast the Breitenbush anticline extends from Mt. Hood to south of the landslide. On all sides at an average of 7.5km from the landslide are four normal faults.

SAMPLING & METEORLOGICAL METHODS

On March 4th, 2016 I collected 12 water samples from a combination of surface flow, Silt Creek, and springs throughout the landslide over 200m of vertical relief (Figure 3). Samples were taken from as high as 300m below the main head scarp down to the confluence of Silt Creek and Thomas Creek at the toe of the landslide. Sampling from higher elevations up to the main head scarp was not possible as concerns about instability were present and demarcated off-limits by Weyerhaeuser. Surface flow and Silt Creek samples were sealed in glass jars to isolate atmospheric exchange and to allow for settling of suspended sediments. Spring water samples were clear and free of suspended sediments therefore these were placed directly into 2mL auto sampling vials and sealed onsite to isolate any atmospheric exchange. All samples were placed into 2mL auto sampling vials and submitted to UC Davis Stable Isotope Facility for analysis of ^{18}O and D/H isotope ratios and compared against IAEA (International Atomic Energy Agency) standard reference of VSMOW (Vienna Standard Mean Ocean Water). VSMOW is an international measurement standard for stable isotope analysis that provides the values of $\delta^{18}O$ and $\delta^{2}H$ in ocean water as a baseline (Coplen, 1996). These analyses were used to establish the sample's elevation source and to compare the composition against well-established standards. The $\delta^{18}O$ value is is defined as $\delta^{18}O = (R_{sample}/R_{standard} - 1) *1000$, where R_{sample} is the ratio of ^{18}O to ^{16}O in the sample, and $R_{standard}$ is the same, but for VSMOW. This equation is also used for δD (Deuterium 'D') values for the isotopic ratios of H and ^{2}H.

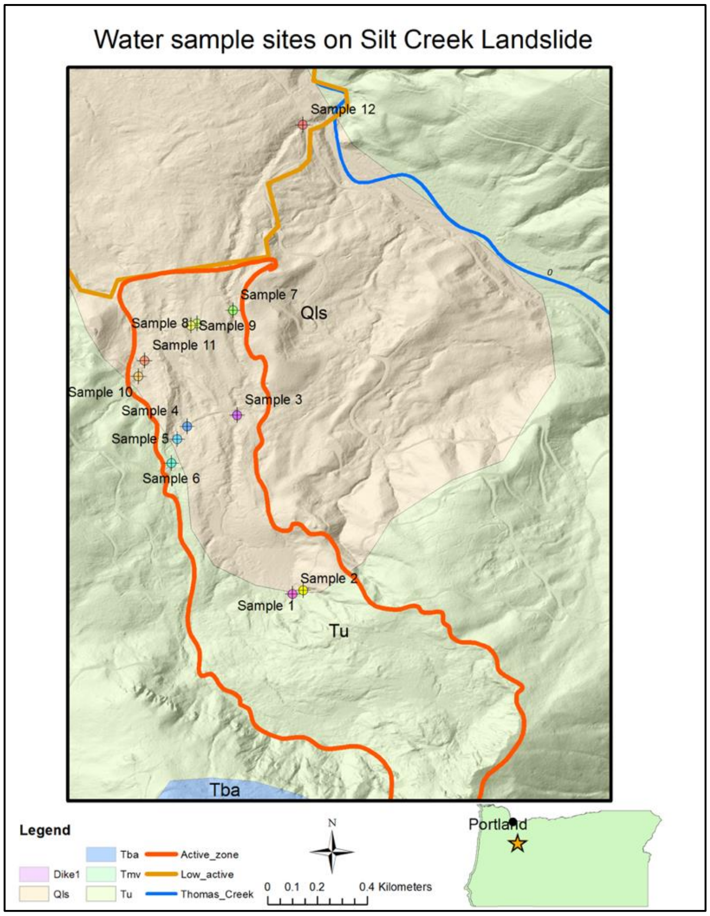

Figure 3. Geologic location map of water samples. Samples 1-3, 6, 7, 10, & 12 were obtained from surface water while samples 4, 5, 8, & 9 were from springs. Geologic units are: Quaternary landslide deposits (Qls)

In the Northwest for example, on the windward side of the Cascades precipitation occurs as mid-latitude cyclones, formed over the Pacific Ocean, which migrate eastward and experience orographic uplift. During uplift the cyclones experience cooler temperatures and as such the dew point is reached resulting in precipitation. ^{18}O is a heaver isotope than ^{16}O and is therefore preferentially condensed resulting in an enrichment of ^{18}O in precipitation. Hence lower elevations experience greater levels of ^{18}O in precipitation. The net result is that higher elevations have depleted values of ^{18}O. By comparing the $^{18}O/^{16}O$ ratio ($\delta^{18}O$) against a well-established "altitude-isotope" profile (Jefferson, 2006) the elevation at which groundwater was recharged can be estimated. Brooks et al. (2012) have developed the most extensive empirical relationship between $\delta^{18}O$ values and recharge elevation for the Northwestern US by the following equation:

$$\delta^{18}O = -0.0028x - 8.05 \qquad (1)$$

where x is recharge elevation in meters. Natural variability from this linear trend is approximately ± 1.5 per mill. Other studies have determined this relationship and are in general agreement with the equation of the linear fit varying from $\delta^{18}O = -0.0016x-10.57$ (Jefferson et al., 2006) to $\delta^{18}O=-0.0018x-10.9$ (James et al., 2000).

The global meteoric water line (GMWL) is a plot of δD vs $\delta^{18}O$ of ocean water that follows the following linear relationship (Craig, 1961):

$$\delta D = (8 * \delta^{18}O) + 10 \qquad (2)$$

Deviations in the slope for local meteoric water lines (LMWL) can be used to infer the amount of evaporation that has occurred (Gat, 1981). For example, under low humidity conditions the slope of δD should be lower than the 8 of the GMWL, which can be an indication that high evaporation conditions existed.

To provide a meteorological context, make an additional estimate of the transit time for precipitation to reach the landslide's failure plane, and to understand the conditions leading up to reactivation, an analysis of precipitation events and volumes was conducted following an Iverson et al. (2015). The analysis involved gathering precipitation totals and duration of precipitation events from NOAA station LaComb at an elevation of 177m and 20.5km away from the study site. Comparing the recurrence intervals for different windows of time preceding the landslide reactivation in 2014 to historical values will aid in identifying wetter or drier periods with different timescale leading up to and during the activation of the landslide. I hypothesized that the timescale associated with the wettest period leading up to the landslide reactivation would provide an order of magnitude estimation of the transit time for precipitation to enter the recharge area and travel through the groundwater system to reach the landslide failure plane.

RESULTS

To provide an accurate estimation of the average water recharge elevation for each sample collected, I delineated the watershed corresponding to each to water sample by using the Hydrology Tools in ArcMap (Figure 4). Based on this, the average watershed elevation was determined for each sample and $\delta^{18}O$ was plotted against these elevations (Figure 5). The isotopic results and mean watershed elevations of the samples located in Figure 3 are listed in Table 1. Values of δD values range from a -70.0‰ to -65.1‰ and $\delta^{18}O$ values range from -10.57‰ to -9.83‰, while sample elevations ranged from 503 to 739m, a range of 236m. These samples plot slightly above the Global Meteoric Water Line (GMWL) (Figure 6). The slope of the LMWL of 5.56 is markedly lower than that of the GMWL slope of 8, and the two lines converge at a value of -8.339 $\delta^{18}O$. A plot of $\delta^{18}O$ values vs. average watershed and spring elevations (Figure 5), does not show a negative slope as predicted for the Western Cascades (Jefferson, 2006 & James et. al., 2000), and instead shows variability around a mean value of -10.09, which is comparable to the analytical error of each sample of 0.13 for $\delta^{18}O$. Therefore, no trend in $\delta^{18}O$ as a function of recharge elevation could be ascertained. Instead, these values are consistent with local meteoric water that falls during winter storms at similar elevations in the Western Cascades (Brooks et. al., 2010).

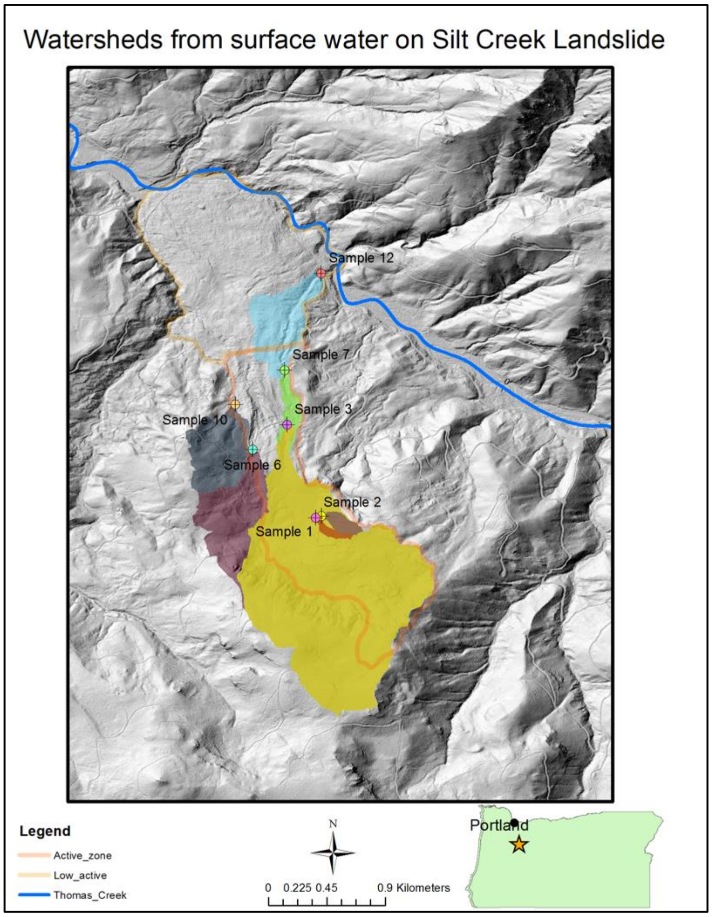

Figure 4. LiDAR map of watersheds, shown in different semi-transparent colors, of surface water samples. Outline of landslide in pale orange & yellow. Watersheds for samples #3,7,12 overlap, such that the entire area of watershed 3 (yellow) is contained within watershed 7(green), both of which are contained within watershed 12 (blue). Blue line represents Thomas Creek.

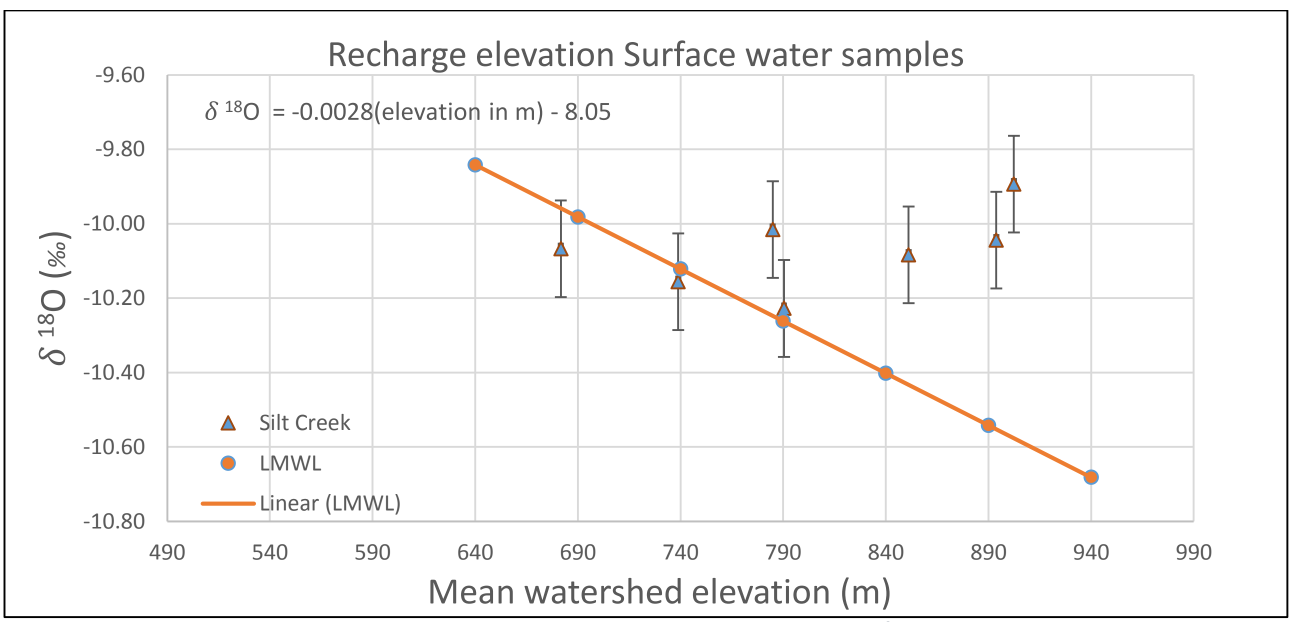

Figure 5. Recharge elevation based on mean watershed elevation of Silt Creek samples. $\delta^{18}O$ values are expressed in per mill (‰) as a function of elevation in meters. The Local Meteoric Water Line (LMWL) are from results of isotopic fractionation of the

Willamette River Basin completed by Brooks (2012). The expected relationship is lighter isotopes (i.e. more negative $\delta^{18}O$) occur at higher elevations. Deviations from this can provide insights into localized particularities.

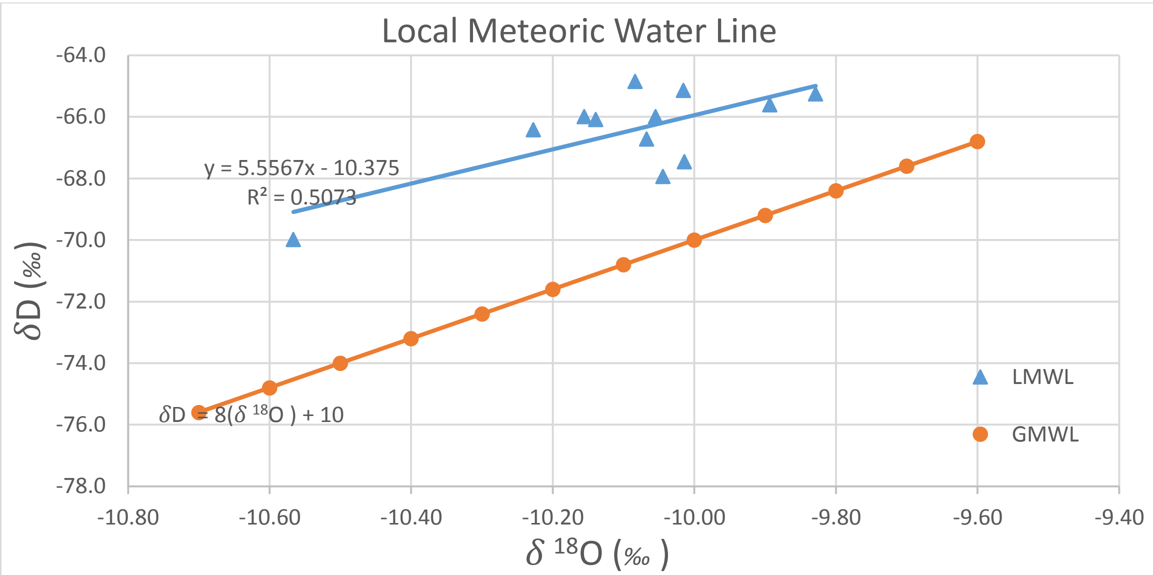

Figure 6. Silt Creek samples (Local Meteoric Water Line (LMWL)) of both surface water and springs, plotted as blue triangles, compared against the Global Meteoric Water Line (GMWL) (Craig, 1961), plotted as orange dots. $\delta^{18}O$ and δD are expressed in per mill (‰). Comparing local sources against the GMWL can provide insights into the atmospheric condition affecting localized water systems.

Table 1. Isotopic and physical data for Silt Creek Landslide samples. Sample elevation is the exact elevation that sample was taken. Average Watershed Elevation refers to ArcMap calculated average elevation of the watershed feeding into sample location. Spring sources lack Average Watershed Elevation as ArcMap hydrology tools are limited to surface flow. VSMOW refers to Vienna Standard Mean Ocean Water and is an international reporting standard for stable isotopes.

SAMPLE ID	SOURCE	SAMPLE ELEVATION (M)	AVG. WATERSHED ELEVATION (M)	VSMOW δD (‰)	VSMOW δ^{18}O (‰)
1	Surface	739	790.4	-66.4	-10.23
2	Surface	721	785.0	-65.1	-10.02
3	Surface	639	902.4	-65.6	-9.89
4	Spring	636	NA	-70.0	-10.57
5	Spring	645	NA	-65.3	-9.83
6	Surface	645	738.9	-66.0	-10.16
7	Surface	598	893.8	-67.9	-10.04
8	Spring	621	NA	-66.0	-10.06
9	Spring	620	NA	-66.1	-10.14
10	Surface	604	681.7	-66.7	-10.07
11	Spring	602	NA	-67.5	-10.01
12	Surface	503	851.1	-68.4	-10.08

Meteorological analysis of precipitation data gathered from 1973 to 2014 (Figure 7) at the LaComb weather station operated by the USGS at an elevation of 158.5m at a distance of

20.7km SW of the landslide (Figure 1) are provided in Table 2. The estimated date of landslide reactivation is assumed to have occurred sometime within the month of July. Therefore, for the duration of days preceding reactivation the greatest amount of precipitation that ended within the month of July was ascertained and compared against all other similar durations over the 42-year span. For example, the greatest 30-day precipitation total that concluded within July 2014 was 57.15mm ending on July 13. This total was greater than 31% of 30-day periods throughout the 42 years. For comparison the greatest 30-day precipitation was 586.74mm that ended on 12/21/2006. Total precipitation measured over time periods ranging from 1 week to 3 years tended to be near or lower than average leading up to the landslide reactivation, while precipitation measured over the 4 to 5 years leading up to the reactivation was above average.

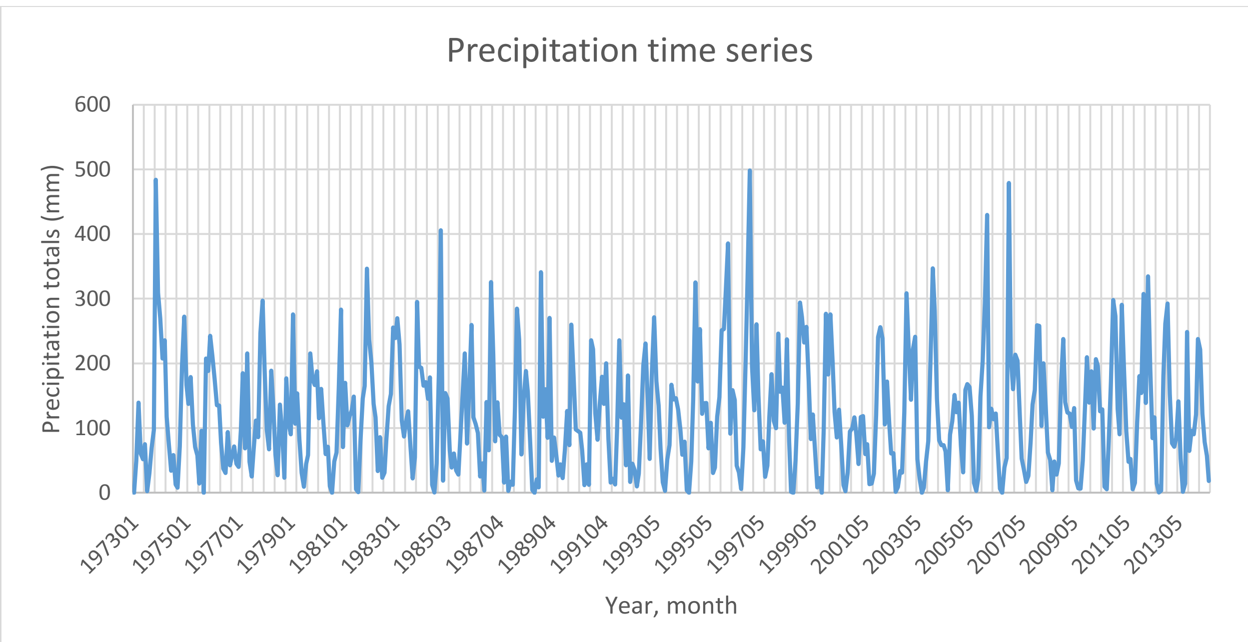

Figure 7. Precipitation total over 42-year period at LaComb weather station. Precipitation totals are in mm. Dates are listed as year followed by month number. For example, 197301 is Janurary 1973. Date interval is every 24months. Note the cyclic pattern of high and low precipitation totals. Winter season experiences the greatest totals while summer experiences the lowest.

Table 2. Meteorological analysis of precipitation totals from LaComb weather station over a 42-year period from 1973 to 2014. Duration of precipitation that ended during the month of reactivation, July 2014, were compared against all similar durations

over the 42-year span. For example, the greatest 30-day precipitation total that concluded within July 2014 was 57.15mm ending on July 13. This total was greater than 31% of all 30-day periods throughout the 42 years.

Precipitation ending in July 2014				Greatest Precipitation on Record	
Duration of precipitation period (days)	Precipitation total (mm)	Ending date of precipitation period in July 2014	Prior precipitation totals exceeded	Greatest Precipitation (mm)	Ending date of greatest precipitation
7	32.77	7/1/2014	67%	250.44	11/08/2006
10	34.04	7/3/2014	56%	281.94	11/11/2006
14	47.75	7/1/2014	53%	365.76	11/22/2006
30	57.15	7/13/2014	31%	586.74	12/21/2006
45	76.45	7/2/2014	25%	842.52	01/09/2007
60	135.38	7/3/2014	32%	896.11	01/12/1997
180	833.37	7/1/2014	67%	1671.83	04/16/1974
1,2,3,4,5 year precipitation ending July 31, 2014					
365	1368	7/31/2014	39%	2014.9	07/30/1997
730	2685.5	7/31/2014	50%	3558.2	7/30/1998
1095	4336.2	7/31/2014	62%	5251.6	7/30/1999
1460	6055.2	7/31/2014	90%	7076.8	7/30/1998
1825	7546.3	7/31/2014	75%	8770.2	7/30/1999

DISCUSSION

Surface water samples from the landslide have similar δ^{18}O values across the 230m range of elevations (Figure 5), and these values are consistent with local meteoric water. This implies that the surface water and springs on the landslide are not being supplied with water from higher elevations above the landslide complex. Instead, the landslide's groundwater recharge area might be confined to the areal extent of the landslide itself. Below, I discuss physical process that may have caused the isotopic composition of my samples to differ from previously determined local and global meteoric water lines, and suggest a conceptual model for groundwater recharge and flow within the landslide complex consistent with the measured isotopic values.

As documented by Brooks (2012) and Jefferson (2006) the Willamette Basin experiences an enrichment of the 'lighter' oxygen isotope in precipitation at higher elevations such that δ^{18}O values become more negative. In those studies, samples were obtained over years and covered a large geographic area such that there was enough differentiation in results. The deviation of my samples from expected values may be the result of one or more of the following: a small range of sample elevations, the effect of evaporation, seasonal variability in $\delta^{18}O$ fractionation, and atmospheric conditions at time of sampling.

At the time of sampling the uppermost portion of the head scarp was inaccessible limiting the sampling vertical relief to 236 m. Comparing Figure 6 with the non-evaporated results from Brooks (2012) in Figure 8, 236 m of relief corresponds to a predicted change in the mean $\delta^{18}O$ values that is small compared to the natural variability at an elevation of ~800 m, which ranges approximately -11‰ to -8.5‰. Brooks' values occur over the entire Willamette River Basin over a 2-year period. Given that my values are from a single sampling session at one location it is reasonable that my results fall within the natural variability of $\delta^{18}O$ values over a narrow elevation range. Furthermore, the mean $\delta^{18}O$ value of -10.09‰ across the landslide is wholly in-line with the regional values.

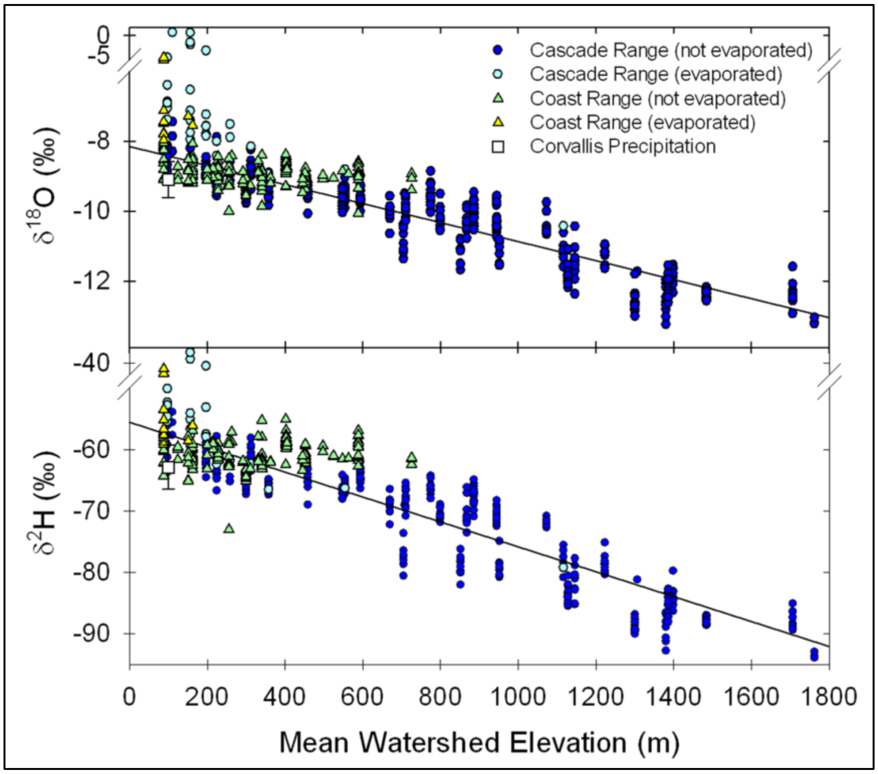

Figure 8. Plot of variations of stable isotopes O & H (Brooks, 2012). The blue dots of Cascade Range (not evaporated) are of comparable data. $\delta^{18}O$ and δD are expressed in per mille (‰). By comparing this plot to the results in Figure 6 the mean values of $\delta^{18}O$ (-10.09‰ $\delta^{18}O$) conform to regional expectations of the Western Cascades.

Samples in Figure 6 were sourced from surface flow from just below the internal head scarp to the confluence of Silt Creek and Thomas Creek. Surface flow appears to be sourced from water emanating from the wall of the internal head scarp, below which it forms braided streams throughout the middle section of the landslide. From there it coalesces into the main trunk of Silt Creek. Previous reconnaissance of the area identified a pool of water behind the internal head scarp. It is this pool of water that may be the main contributor for the current Silt Creek and groundwater, and if so, could be the reason for the similar oxygen isotope values across elevation. Furthermore, the deuterium-oxygen isotope relationship plots higher and with a lower slope than that of the GMWL. This may be an indication that evaporation has occurred (Gat, 1981) (Figure 9) as the lighter isotopes are preferentially evaporated.

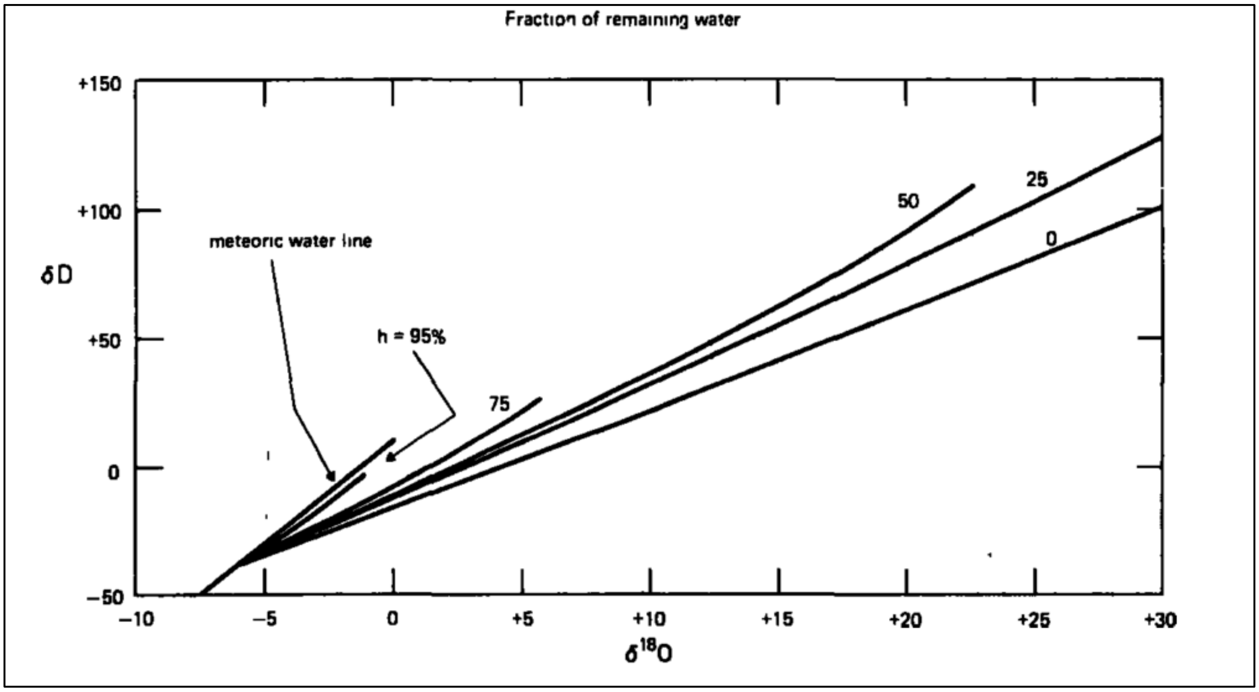

Figure 9. Departures from the GMWL with lower slopes indicate evaporation has occurred (Gat, 1981). δ^{18}O and δD are expressed in per mille (‰). The lower the slope the greater the evaporation and lower the humidity the body of water experienced. By comparing this plot to Figure 6 the water sample may have experienced some evaporation.

The deviation of oxygen isotope values in figure 6 off the GMWL trend may also be result of seasonal variation. The NW coast of North America has its lowest δ^{18}O values during the winter, of approximate range of -11.25‰ to -10.25‰, and highest during the summer, of approximate range of -8‰ to -8.5‰. (Figure 10)(IAEA, 2016) Sampling took place during March, and the mean δ^{18}O of -10.09‰ is consistent with that of early spring precipitation (Figure 10.)

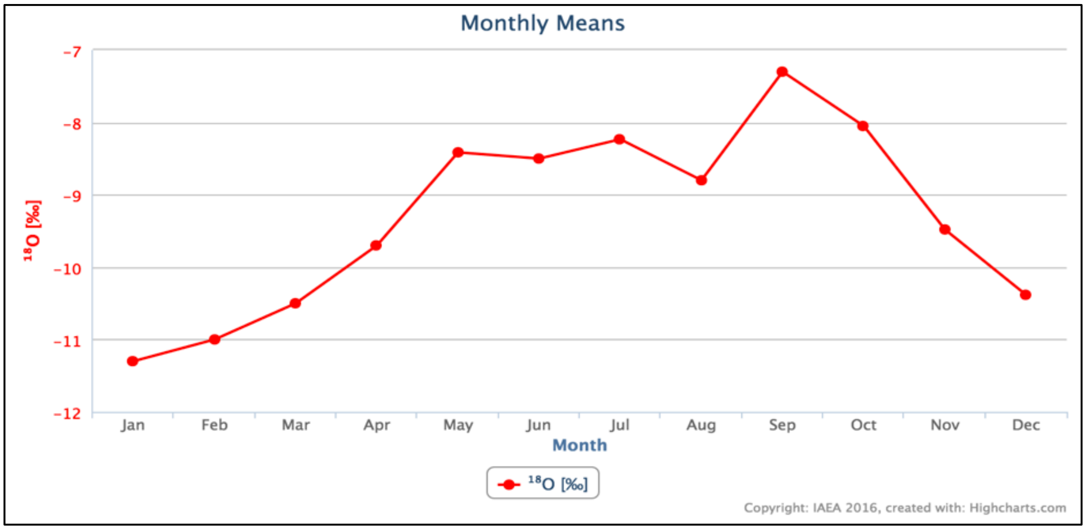

Figure 10. Plot of monthly variability in $\delta^{18}O$ values from Victoria, BC (IAEA, 2016). $\delta^{18}O$ are expressed in per mille (‰). For the west coast of N. America $\delta^{18}O$ are heaviest, i.e. least negative, during the summer, and lightest during the winter.

The atmospheric conditions on the day of sampling had 0.76 mm of precipitation, 89% humidity, and a high of 16 degrees Celsius. Precipitation occurred throughout the sampling area and mixed with surface flow. While the GMWL is an average of stable isotope values over time and space, the results of my samples for Figure 5 reflect only the surface water available that day. There is a strong possibility that any groundwater signal present was obscured by the influx of local precipitation.

The precipitation totals preceding the reactivation of the Silt Creek landslide in the short range (7-180 days) that concluded within July 2014 exceeded 25% to 67% of similar durations over the entire 42-year period. For the long range (one to five years), precipitation totals exceeded 39% to 90%. It is challenging to relate the short duration precipitation events to the reactivation in part because the exact date of reactivation is unknown. Furthermore, these short duration precipitation events are not atypically high, as was observed, for example, preceding the Oso Landslide (Iverson, 2015). For comparison, the largest short duration precipitation values occurred in 1974, 1997 2006, and 2007, which I assume too far removed from reactivation to have any influence on this landslide. The low to average values for time periods of 1 week to three years document the drought to drought-like conditions experienced in western Oregon between 2012 and 2014. On the other hand, the total precipitation for the most recent 4 years exceeded 90% of all other four-year precipitation totals and may suggest the timescale for the landslide to respond to fluctuations in precipitation. Further investigation is needed to ascertain whether or not this is the case. The greatest precipitation totals in the record occurred in the 1997/1998 winter, and are not likely to have had a direct influence on the reactivation.

The landslide occurred within a formation that is poorly welded and composed of tuffaceous materials that weather readily to clay minerals and capped by resistant flows of basalt. Aerial photos dating as far back as 1994 and as recent as 2011 show indications that this specific location is prone to sliding, and its morphology suggests that the landslide complex is much older. Landslide movement tends to align platy clay minerals along the failure plane, such that hydraulic conductivity is reduced resulting in an impermeable layer and a perched aquifer (Baum and Reid, 1995). In this conceptual model, which has been documented for a clay-rich landslide in Hawaii (Baum and Reid, 1995), any water that infiltrates the surface of the landslide collects along its base and contributes to a reduction in frictional strength of the shear zone. Similarly, water infiltrating outside the landslide would remain isolated from the water within the landslide, which is consistent with our isotopic results. This ‘bathtub’ model is a plausible cause of failure on Silt Creek, and may be the reason for failure during the dry summer months.

CONCLUSIONS

This investigation used isotopic analysis of surface water and analysis of precipitation records to determine the relationship between landslide initiation and groundwater at a western Cascades landslide. The Silt Creek Landslide reactivated during the summer of 2014 in the midst of state-wide drought-like conditions that existed for the previous two years. Since then the slide has continued to move at a relatively high rate of ~15m/yr. The location of the slide occurs within a formation that is poorly welded and composted of tuffaceous materials that readily weather to clay minerals and are capped by resistant flows of basalt. LiDAR imagery has shown that several other landslides have occurred in the valley indicating that the entire upper Thomas Creek Watershed is unstable and prone to failure. This will likely continue as fluvial incision continues to undercut and over-steepen structurally unstable slopes. For this particular landslide groundwater and surface flow likely does not originate from higher elevations, as suggested by the oxygen isotope results. Instead the isotopic signature indicates a source of local meteoric water that has been subjected to evaporation. Ponded water below the landslide's head scarp is therefore a plausible source for groundwater and surface flow further down the landslide. Precipitation records highlight the dry conditions that existed for up to 3 years before reactivation, suggesting that instead of a storm driven trigger, precipitation may have contributed to the accumulation of groundwater within the landslide complex over a longer time scale. The local geologic conditions and areas of groundwater infiltration support the proposed "bathtub model" of landslide hydrology, which may be a mechanism for this landslide's continued reactivation. Identifying what specifically triggers a slope failure can be challenging, and this study suggests that analysis of stable isotopes in surface water at high spatial and temporal resolution may provide useful clues to pinpoint hydrologic triggering mechanisms.

REFERENCES

Baum, R.L., and Reid, M.E., 1995, Geology, hydrology, and mechanics of a slow-moving, clay-rich landslide, Honolulu, Hawaii: GSA Reviews in Engineering Geology, v. X.

Brooks, J.R., Wigington, P.J., Phillips, D.L., Comeleo, R., and Coulombe, R., 2012, Willamette River Basin surface water isoscape (δ^{18}O and δ^{2}H): temporal changes of source water within the river: Ecosphere, v. 3, p. art39, doi: 10.1890/ES11-00338.1.

Coplen, T.B., 1996, New guidelines for reporting stable hydrogen, carbon and oxygen isotope-ratio data: Geochim. et Cosmochim. Acta, v. 60, p. 3359–3360.

Craig, H., 1961, Isotope variations in meteoric waters: Science, v. 133, p. 1702–1703.

Cruden, D.M., 1996, Cruden,D.M., Varnes, D.J., 1996, Landslide Types and Processes, Special Report , Transportation Research Board, National Academy of Sciences, 247:36-75: Special Report - National Research Council, Transportation Research Board, v. 247, p. 76.

Gat, J.R., and Gonfiantini, R., 1981, Stable isotope hydrology: 356 p.

Hammond, P.E., 1976, DOGAMI Open-File Report O-76-05, Preliminary report on the reconnaissance geology of the Upper Clackamas and North Santiam rivers area, Cascade Range, Oregon:.

Iverson, R.M., George, D.L., Allstadt, K., Reid, M.E., Collins, B.D., Vallance, J.W., Schilling, S.P., Godt, J.W., Cannon, C.M., Magirl, C.S., Baum, R.L., Coe, J.A., Schulz, W.H., and Bower, J.B., 2015, Landslide mobility and hazards: Implications of the 2014 Oso disaster: Earth and Planetary Science Letters, v. 412, p. 197–208, doi: 10.1016/j.epsl.2014.12.020.

James, E.R., Manga, M., Rose, T.P., and Hudson, G.B., 2000, The use of temperature and the isotopes of O, H, C, and noble gases to determine the pattern and spatial extent of groundwater flow: Journal of Hydrology, v. 237, p. 100–112, doi: 10.1016/S0022-1694(00)00303-6.

Jefferson, A., Grant, G., and Rose, T., 2006, Influence of volcanic history on groundwater patterns on the west slope of the Oregon High Cascades: Water Resources Research, v. 42, p. W12411, doi: 10.1029/2005WR004812.

Lambe, W.T. and Whitman, R.V., 1969, Soil Mechanics: New York, John Wiley & Sons, 548p p.

Lu, N. Godt, J.W., 2013, Hillslope Hydrology and Stability: Cambridge University Press,.

Orr, E.L., and Orr, W.N., 2012, Oregon Geology: Corvallis, Or, Oregon State University Press, 304 p.

Ritter, D.F., Kochel, R.C., and Miller, J.R., 2011, Process Geomorphology: Long Grove, Illinois, Waveland Press, Inc., 652 p.

Schuster, R.L., 1996, Socioeconomic effects of landslides, in Turner, A. K.,: Transportation Research Board Special Report 247,.

Terzaghi, K., 1950, Terzaghi_Mechanism of landslides_1950.pdf:.

Thayer, T., 1939, Geology of the Salem Hills and the North Santiam River Basin, Oregon:.

Walker, G.W. and MacLeod, N.S., 1991, Geologic map of Oregon: U.S. Geological Survey, v. scale 1:50.

Wells, R.E., and Simpson, R.W., 2001, Northward migration of the Cascadia forearc in the northwestern U.S. and implications for subduction deformation: Earth, Planets and Space, v. 53, p. 275–283, doi: 10.1186/BF03352384.

White, C.M., 1980, Geology of the Bretienbush Hot Springs Quadrangle, Oregon: Oregon Department of Geology and Mineral Industries Special Paper 9, p. 26.